

Comparison of Two Couplings of the Finite Volume Method and the Boundary Element Method

Christoph Erath

Abstract In many fluid dynamics problems the boundary conditions may be unknown, or the domain may be unbounded. Also mass conservation and stability with respect to dominating convection is substantial. Therefore, we test two coupling methods to address these issues on the prototype of a flow and transport problem. More precisely, we couple the vertex-centered and the cell-centered finite volume method with the boundary element method, FVM-BEM and CFVM-BEM, respectively. Also robust refinement indicators are considered which allow us to steer an adaptive mesh-refinement algorithm to treat efficiently problems with singularities or boundary/internal layers—shown on two examples.

1 Model Problem and Notation

Due to the conservation of mass property and a stable approximation for convection dominated problems finite volume methods are well established in fluid dynamics. Boundary element methods can be used if the fundamental solution of the problem is known. Since they reduce the approximation problem from a domain to its boundary, they can be employed for problems on unbounded domains (with radiation conditions) without truncating the domain. In a sense they also feature local conservation. Two coupling methods of both schemes are considered here to benefit and merge their properties. In an interior domain $\Omega \subset \mathbb{R}^d$ ($d = 2, 3$), which is a bounded and simply connected domain with polygonal/polyhedral Lipschitz boundary Γ , we consider the prototype of a flow and transport problem and discretize it with a FVM. Whereas in the corresponding unbounded exterior domain $\Omega_e = \mathbb{R}^d \setminus \overline{\Omega}$ we approximate a diffusive process with the BEM. Special care has to be taken on the so called

C. Erath (✉)

Department of Mathematics, University of Vienna, Oskar-Morgenstern-Platz 1,
Vienna 1090, Austria
e-mail: christoph.erath@univie.ac.at

coupling boundary $\Gamma = \partial\Omega = \partial\Omega_e$, which is divided in an inflow and outflow part, namely $\Gamma^{in} := \{x \in \Gamma \mid \mathbf{b}(x) \cdot \mathbf{n}(x) < 0\}$ and $\Gamma^{out} := \{x \in \Gamma \mid \mathbf{b}(x) \cdot \mathbf{n}(x) \geq 0\}$, respectively. Here \mathbf{n} is the normal vector on Γ pointing outward with respect to Ω . The mathematical formulation of our problem reads: Find u and u_e such that

$$\operatorname{div}(-\alpha \nabla u + \mathbf{b}u) + \gamma u = f \quad \text{in } \Omega, \tag{1a}$$

$$\Delta u_e = 0 \quad \text{in } \Omega_e, \tag{1b}$$

$$u_e(x) = a_\infty + b_\infty \log|x| + o(1) \quad \text{for } |x| \rightarrow \infty, d = 2, \tag{1c}$$

$$u_e(x) = \mathcal{O}(|x|^{-1}) \quad \text{for } |x| \rightarrow \infty, d = 3, \tag{1d}$$

$$u = u_e + u_0 \quad \text{on } \Gamma, \tag{1e}$$

$$(\alpha \nabla u - \mathbf{b}u) \cdot \mathbf{n} = \frac{\partial u_e}{\partial \mathbf{n}} + t_0 \quad \text{on } \Gamma^{in}, \tag{1f}$$

$$(\alpha \nabla u) \cdot \mathbf{n} = \frac{\partial u_e}{\partial \mathbf{n}} + t_0 \quad \text{on } \Gamma^{out}. \tag{1g}$$

In the two dimensional case we can fix either $a_\infty \in \mathbb{R}$ or $b_\infty \in \mathbb{R}$; see [1]. The given data satisfy $f \in L^2(\Omega)$, $u_0 \in H^{1/2}(\Gamma)$ and $t_0 \in L^2(\Gamma)$, where $L^m(\cdot)$ and $H^m(\cdot)$, $m > 0$, denote the standard Lebesgue and Sobolev spaces equipped with the usual norms $\|\cdot\|_{L^2(\cdot)}$ and $\|\cdot\|_{H^m(\cdot)}$, respectively. The diffusion coefficient α is positive, and there holds $(\operatorname{div} \mathbf{b})/2 + \gamma \geq C_1 \geq 0$ and $\|\operatorname{div} \mathbf{b} + \gamma\|_{L^\infty(\Omega)} \leq C_2 C_1$ with the constants $C_1, C_2 \geq 0$ for the convection vector function $\mathbf{b} \in W^{1,\infty}(\Omega)^d$ (vector of Lipschitz continuous functions) and the reaction function $\gamma \in L^\infty(\Omega)$.

It is shown in [1] that in a weak sense there exists a unique solution $u \in H^1(\Omega)$ and $u_e \in H^1_{loc}(\Omega_e)$ (set of all local H^1 -functions) of the model problem (1). Although not explicitly stated in [1] the result is also valid (verbatim) for the 3-D case. The proof is based on the fact that we can transform the unbounded exterior problem (1b)–(1d) into an integral equation—the exterior Calderón system—with the Cauchy data $\xi := u_e|_\Gamma \in H^{1/2}(\Gamma)$ and $\phi := \partial u_e / \partial \mathbf{n}|_\Gamma \in H^{-1/2}(\Gamma)$. The weak form of this system and the interior weak form are coupled through the conditions (1e)–(1g). For more details we refer to [1] and only remark that the Calderón system is based on some bounded and linear integral operators $\mathcal{V} \in L(H^{s-1/2}(\Gamma); H^{s+1/2}(\Gamma))$ (single layer op.), $\mathcal{K} \in L(H^{s+1/2}(\Gamma); H^{s+1/2}(\Gamma))$ (double layer op.), $\mathcal{K}^* \in L(H^{s-1/2}(\Gamma); H^{s-1/2}(\Gamma))$ (adjoint double layer op.) and $\mathcal{W} \in L(H^{s+1/2}(\Gamma); H^{s-1/2}(\Gamma))$ (hypersingular integral op.) for $s \in [-1/2, 1/2]$. These operators are based on the fundamental solution $-\frac{1}{2\pi} \log|x|$ for the 2-D case and $\frac{1}{4\pi} \frac{1}{|x|}$ for the 3-D case of the exterior problem; for more details see e.g. [1].

Triangulation: To simplify notation and the language we only note the construction for the 2-D case. Throughout, \mathcal{T} denotes a triangulation, the *primal mesh*, of Ω , where \mathcal{N} and \mathcal{E} are the corresponding set of nodes and edges, respectively. The notation in this work is consistent in the sense that \mathcal{N}_I and \mathcal{N}_Γ denote the set of nodes in the interior and on the boundary, respectively, $\mathcal{E}_\Gamma^{in} \subset \mathcal{E}_\Gamma$ denotes all coupling edges on Γ^{in} , \mathcal{E}_T all edges of T , and so on. For brevity, the elements $T \in \mathcal{T}$ are

non-degenerated triangles. The Euclidean diameter of $T \in \mathcal{T}$ is $h_T := \sup_{x,y \in T} |x - y|$ and h_E denotes the length of an edge $E \in \mathcal{E}$. The triangulation is regular, i.e., the ratio h_T of any element $T \in \mathcal{T}$ to the diameter of its largest inscribed ball is bounded by a constant independent of h_T . Additionally, we assume that the triangulation \mathcal{T} is aligned with the discontinuities (if any) of any given data, and \mathbf{n} denotes the unit normal vector to the boundary pointing outward the domain.

Dual mesh: If we connect the center of gravity of an element $T \in \mathcal{T}$ with the midpoints of the edges $E \in \mathcal{E}_T$ we get the *dual mesh* \mathcal{T}^* with its boxes $V \in \mathcal{T}^*$. A box associated with a vertex $a_i \in \mathcal{N}$ (from the primal mesh, $i = 1 \dots \#\mathcal{N}$, which lies in the box) is denoted by $V_i \in \mathcal{T}^*$. Note that this vertex is unique.

We denote by $\mathcal{C}(\cdot)$ all continuous functions. The L^2 scalar product is $(\cdot, \cdot)_\omega$, $\omega \subset \Omega$. The duality between $H^m(\Gamma)$ and $H^{-m}(\Gamma)$ is given by the extended L^2 -scalar product $(\cdot, \cdot)_\Gamma$. Moreover, we define the piecewise affine and globally continuous function space on \mathcal{T} by $\mathcal{S}^1(\mathcal{T}) := \{v \in \mathcal{C}(\Omega) \mid v|_T \text{ affine for all } T \in \mathcal{T}\}$ and the piecewise constant space on \mathcal{T} by $\mathcal{P}^0(\mathcal{T}) := \{v \in L^2(\Omega) \mid v|_T \text{ const. for all } T \in \mathcal{T}\}$. The spaces $\mathcal{S}^1(\mathcal{E}_\Gamma)$, $\mathcal{P}^0(\mathcal{E}_\Gamma)$, and $\mathcal{P}^0(\mathcal{T}^*)$ are equivalently defined as above and $\mathcal{S}_*^1(\mathcal{E}_\Gamma)$ is $\mathcal{S}^1(\mathcal{E}_\Gamma)$ with integral mean zero over \mathcal{E}_Γ .

2 FVM (Vertex-Centered) and BEM Coupling

A detailed description and motivation of this type of coupling can be found in [1]. The discrete system reads for $a_\infty = 0$: Find a discrete solution $u_h \in \mathcal{S}^1(\mathcal{T})$, $\xi_h \in \mathcal{S}_*^1(\mathcal{E}_\Gamma)$ and $\phi_h \in \mathcal{P}^0(\mathcal{E}_\Gamma)$ of our model problem such that

$$\mathcal{A}_V(u_h, v^*) - (\phi_h, v^*)_\Gamma = F(v^*), \quad (2a)$$

$$-\langle u_h, \psi_h \rangle_\Gamma - \langle \mathcal{V} \phi_h, \psi_h \rangle_\Gamma + \langle (1/2 + \mathcal{K}) \xi_h, \psi_h \rangle_\Gamma = -\langle u_0, \psi_h \rangle_\Gamma, \quad (2b)$$

$$\langle (1/2 + \mathcal{K}^*) \phi_h, \theta_h \rangle_\Gamma + \langle \mathcal{W} \xi_h, \theta_h \rangle_\Gamma = 0 \quad (2c)$$

for all $v^* \in \mathcal{P}^0(\mathcal{T}^*)$ ($v^* := \sum_{x_i \in \mathcal{N}} v_i^* \chi_i^*$, $v_i^* \in \mathbb{R}$), $\theta_h \in \mathcal{S}_*^1(\mathcal{E}_\Gamma)$, $\psi_h \in \mathcal{P}^0(\mathcal{E}_\Gamma)$. The bilinear form \mathcal{A}_V and the right-hand side $F(v^*)$ are defined as

$$\begin{aligned} \mathcal{A}_V(u_h, v^*) &:= \sum_{a_i \in \mathcal{N}} v_i^* \left(\int_{\partial V_i \setminus \Gamma} (-\alpha \nabla u_h + \mathbf{b} u_h) \cdot \mathbf{n} \, ds + \int_{V_i} \gamma u_h \, dx + \int_{\partial V_i \cap \Gamma^{out}} \mathbf{b} \cdot \mathbf{n} u_h \, ds \right), \\ F(v^*) &:= \sum_{a_i \in \mathcal{N}} v_i^* \left(\int_{V_i} f \, dx + \int_{\partial V_i \cap \Gamma} t_0 \, ds \right). \end{aligned}$$

Note that the discretization in the interior domain follows along the dual mesh \mathcal{T}^* , u_h approximates u , $\xi_h \approx \xi$, and $\phi_h \approx \phi$ and the two are coupled through ϕ_h in (2a) and u_h in the Calderón system (2b)–(2c). See [1, Remark 3.1] why ξ_h has to be the integral mean. If we want to apply a full upwind scheme for the finite volume scheme, we replace $\mathbf{b} u_h$ in \mathcal{A}_V by its full upwind value $\mathbf{b} u_{h,ij}$. Note that there exists a $\tau_{ij} = V_i \cap V_j \neq \emptyset$ for $V_i, V_j \in \mathcal{T}^*$, i.e., τ_{ij} consists two straight lines and is a

part of ∂V_i and ∂V_j . With $\beta_{ij} := (\int_{\tau_{ij}} \mathbf{b} \cdot \mathbf{n}_i ds) / |\tau_{ij}|$ the upwind value is defined by $u_{h,ij} := u_h(a_i)$ if $\beta_{ij} \geq 0$, and $u_{h,ij} := u_h(a_j)$ otherwise. For a sufficient small mesh size the discrete solution of system (2) and its upwind version exists, is unique, and is of first order; see [1]. This result is also valid for three dimensions.

3 Cell-Centered FVM and BEM Coupling

The CFVM-BEM coupling reads for $a_\infty = 0$: Find $u_h \in \mathcal{P}^0(\mathcal{T})$, $u_{h,\Gamma} \in \mathcal{S}^1(\mathcal{E}_\Gamma)$, $\xi_h \in \mathcal{S}_*^1(\mathcal{E}_\Gamma)$ and $\phi_h \in \mathcal{P}^0(\mathcal{E}_\Gamma)$ such that

$$\sum_{E \in \mathcal{E}_T \setminus \mathcal{E}_\Gamma} F_{T,E}^D(u_h) + \sum_{E \in \mathcal{E}_T \setminus \mathcal{E}_\Gamma^{\text{in}}} F_{T,E}^C(u_h) + F_T^R(u_h) - \int_{\partial T \cap \Gamma} \phi_h ds = \int_T f dx + \int_{\partial T \cap \Gamma} t_0 ds, \quad (3a)$$

$$-u_a + \bar{u}_a + \bar{\zeta}_{a,h} = -\bar{\zeta}_{a,t_0}, \quad (3b)$$

$$-\langle u_{h,\Gamma}, \psi_h \rangle_\Gamma - \langle \mathcal{V} \phi_h, \psi_h \rangle_\Gamma + \langle (1/2 + \mathcal{K}) \xi_h, \psi_h \rangle_\Gamma = -\langle u_0, \psi_h \rangle_\Gamma, \quad (3c)$$

$$\langle (1/2 + \mathcal{K}^*) \phi_h, \theta_h \rangle_\Gamma + \langle \mathcal{W} \xi_h, \theta_h \rangle_\Gamma = 0 \quad (3d)$$

for all $T \in \mathcal{T}$, $a \in \mathcal{N}_\Gamma$, $\theta_h \in \mathcal{S}_*^1(\mathcal{E}_\Gamma)$ and $\psi_h \in \mathcal{P}^0(\mathcal{E}_\Gamma)$. A detailed description of this coupling method can be found in [2]. Note that the discretization in the interior domain follows along the primal mesh \mathcal{T} , u_h approximates u , $\xi_h \approx \xi$, and $\phi_h \approx \phi$. To allow local mesh-refinement we approximate the diffusion flux $F_{T,E}^D(u_h)$ by the diamond path method as in [4]. For the convection flux $F_{T,E}^C(u_h)$ we can choose the full upwind scheme as described in Sect. 2 and $F_T^R(u_h)$ is simply the integral of γ over T . The approximation of u_a is done by an interpolation value \bar{u}_a of certain values u_T of $T \in \mathcal{T}$, see also [4], and a mean value $\bar{\zeta}_a = \bar{\zeta}_{a,h} + \bar{\zeta}_{a,t_0}$. The latter is the approximated conormal of u_e on Γ , which is given by the solution ϕ_h of the boundary element method for the exterior problem and the jump term t_0 . The piecewise affine discrete solution reads $u_{h,\Gamma} := \sum_{a \in \mathcal{N}_\Gamma} u_a \eta_a(x)$ with the standard nodal linear basis function η_a on \mathcal{E}_Γ . Note that the unknown u_a on Γ is also needed for the diamond path. CFVM and BEM are coupled through ϕ_h in (3a) and $u_{h,\Gamma}$ in the Calderón system (3c)–(3d). We want to point out that there is neither an existence proof nor an a priori result available for this type of coupling. Thus, we assume that this systems is well-defined and gives a unique solution.

4 A Posteriori Error Estimator

For convection or reaction dominated problems robust a posteriori estimators are essential. Therefore, we define $\beta_T := \min_{x \in T} \{(\text{div } \mathbf{b}(x))/2 + \gamma(x)\}$ for all $T \in \mathcal{T}$ and $\beta_E := \min \{\beta_{T_1}, \beta_{T_2}\}$ for $E \in \mathcal{E}_I$ with $E \subset T_1 \cap T_2$ or $\beta_E := \beta_T$ for $E \in \mathcal{E}_\Gamma$ with

$E \in \mathcal{E}_T$. Furthermore, we introduce the quantities $\mu_T := \min \{\beta_T^{-1/2}, h_T \alpha^{-1/2}\}$ and $\mu_E := \min \{\beta_E^{-1/2}, h_E \alpha^{-1/2}\}$. We provide an a posteriori estimator of residual type for both coupling schemes, which is based on the primal mesh \mathcal{T} . For the CFVM-BEM the estimator post processes the original piecewise finite volume approximation in the interior domain to a conforming finite element space which leads to the so called Morley interpolant $\mathcal{I}u_h$; see [2]. Let us write $u_{FVM} = u_h$ for FVM-BEM and $u_{FVM} = \mathcal{I}u_h$ for CFVM-BEM. Then the residual reads $R := f - \operatorname{div}(-\alpha \nabla u_{FVM} + \mathbf{b}u_{FVM}) - \gamma u_{FVM}$ and an edge-residual $J : L^2(\mathcal{E}) \rightarrow \mathbb{R}$ is given by

$$J|_E := \begin{cases} (-\alpha \nabla u_{FVM}|_{T'} + \alpha \nabla u_{FVM}|_T) \cdot \mathbf{n} & \text{for all } E \in \mathcal{E}_I, \\ (-\alpha \nabla u_{FVM} + \mathbf{b}u_{FVM}) \cdot \mathbf{n} + \phi_h + t_0 & \text{for all } E \in \mathcal{E}_\Gamma^{in}, \\ -(\alpha \nabla u_{FVM}) \cdot \mathbf{n} + \phi_h + t_0 & \text{for all } E \in \mathcal{E}_\Gamma^{out}, \end{cases}$$

with $E = T \cap T'$, $T, T' \in \mathcal{T}$ for $E \in \mathcal{E}_I$ and $E \in \mathcal{E}_T$ otherwise, and \mathbf{n} pointing outward of T . First we define the refinement indicator for each element $T \in \mathcal{T}$ by

$$\begin{aligned} \eta_T^2 &:= \mu_T^2 \|R\|_{L^2(T)}^2 + \frac{1}{2} \sum_{E \in \mathcal{E}_I \cap \mathcal{E}_T} \alpha^{-1/2} \mu_E \|J\|_{L^2(E)}^2 + \sum_{E \in \mathcal{E}_\Gamma \cap \mathcal{E}_T} \alpha^{-1/2} \mu_E \|J\|_{L^2(E)}^2 \\ &+ \sum_{E \in \mathcal{E}_\Gamma \cap \mathcal{E}_T} h_E \|\partial u_{h,\Gamma} / \partial s - \partial / \partial s (u_0 - \mathcal{V} \phi_h + (1/2 + \mathcal{K}) \xi_h)\|_{L^2(E)}^2 \\ &+ \sum_{E \in \mathcal{E}_\Gamma \cap \mathcal{E}_T} h_E \|\mathcal{W} \xi_h + (1/2 + \mathcal{K}^*) \phi_h\|_{L^2(E)}^2, \end{aligned} \quad (4)$$

where $\partial / \partial s$ denotes the arc length derivative. Note that $u_{h,\Gamma}$ will be replaced by u_h for FVM-BEM. For the upwind FVM-BEM, we additionally define

$$\eta_{T,up}^2 := \alpha_T^{-1/2} \mu_T \sum_{\tau_{ij}^T \in \mathcal{D}^T} \|\mathbf{b} \cdot \mathbf{n}_i (u_h - u_{h,ij}^T)\|_{L^2(\tau_{ij}^T)}^2 \quad (5)$$

for $T \in \mathcal{T}$, where $\mathcal{D}^T := \{\tau_{ij}^T \mid \tau_{ij}^T = V_i \cap V_j \cap T \neq \emptyset \text{ for } V_i, V_j \in \mathcal{T}^* \text{ with } V_i \neq V_j\}$ and $u_{h,ij}^T$ is the upwind value (see Sect. 2). The upper bound is proven in [2, 3] (for FVM-BEM even for the 3-D case) and reads

$$\begin{aligned} C_{\text{rel}}^{-2} (\|u - u_{FVM}\|_\Omega + \|\xi - \xi_h\|_{H^{1/2}(\Gamma)} + \|\phi - \phi_h\|_{H^{-1/2}(\Gamma)})^2 \\ \leq \eta^2 := \sum_{T \in \mathcal{T}} (\eta_T^2 + \eta_{T,up}^2). \end{aligned} \quad (6)$$

The constant C_{rel} depends only on the shape of the elements \mathcal{T} but not on the size, the number of elements or the model data, and

$$\|v\|_{\Omega}^2 := \|\alpha^{1/2}\nabla v\|_{L^2(\Omega)}^2 + \|((\operatorname{div} \mathbf{b})/2 + \gamma)^{1/2}v\|_{L^2(\Omega)}^2 \quad \text{for all } v \in H^1(\Omega)$$

defines the energy (semi)norm. In [2] robustness is also shown against a piecewise constant α . Furthermore, one can also find a proof for a local lower bound of (6) in [2, 3], where the constant additionally depends on the local Péclet number.

5 Numerical Experiments

With the refinement indicators of (4) (plus (5) for FVM-BEM upwinding), we run a standard refinement algorithm with the following criterion: construct a minimal subset $\mathcal{M}^{(k)}$ of $\mathcal{T}^{(k)}$ at step k such that

$$\theta \sum_{T \in \mathcal{T}^{(k)}} (\eta_T^2 (+\eta_{T,up}^2)) \leq \sum_{T \in \mathcal{M}^{(k)}} (\eta_T^2 (+\eta_{T,up}^2))$$

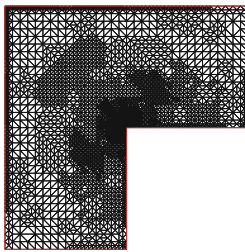
and mark all elements in $\mathcal{M}^{(k)}$ for refinement. We use $\theta = 1/2$ for adaptive mesh-refinement. The shape regularity constant is bounded in all our examples which can be guaranteed by a red-green-blue refinement strategy.

5.1 The Classical L-Shaped Laplace Problem

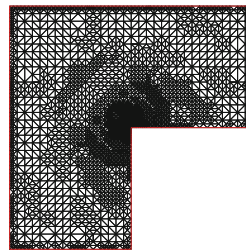
The Laplace problem with $\Omega = (-1/4, 1/4)^2 \setminus ([0, 1/4] \times [-1/4, 0])$ can be seen as a benchmark problem to test discrete systems, especially with adaptive mesh refinement techniques. The given exact solutions read: $u(x_1, x_2) = r^{2/3} \sin(2\varphi/3)$ with $(x_1, x_2) = r(\cos \varphi, \sin \varphi)$ ($r \in \mathbb{R}_0^+, \varphi \in [0, 2\pi[$) for (1a) and for (1b) and (1c) $u_e(x_1, x_2) = \log \sqrt{(x_1 + 0.125)^2 + (x_2 - 0.125)^2}$ with $a_\infty = 0$ and $b_\infty = 1$. The right-hand side is $f = 0$ if we choose $\alpha = 1$, $\mathbf{b} = (0, 0)^T$ and $\gamma = 0$ for our model problem. The jumps u_0 and t_0 are calculated appropriately. We stress that u has a generic singularity at the reentrant corner $(0, 0)$. It is well known that a first order scheme leads to a suboptimal $\mathcal{O}(N^{-1/3})$ order of convergence with respect to the number of elements $N := \#\mathcal{T}$, or $\mathcal{O}(h^{2/3})$ if h denotes the uniform mesh-size. An adaptive refinement algorithm may give us back the optimal order of $\mathcal{O}(N^{-1/2})$. Table 1 shows the energy norm errors starting with a uniform mesh $\#\mathcal{T}^{(0)} = 12$. Note that the (not computable) BEM norms are estimated up to a constant because of $\|\xi - \xi_h\|_{H^{1/2}(\Gamma)}^2 \sim \|\xi - \xi_h\|_{\mathcal{W}}^2 := \langle \mathcal{V}(\xi - \xi_h), \xi - \xi_h \rangle_\Gamma$ and $\|\phi - \phi_h\|_{H^{-1/2}(\Gamma)}^2 \sim \|\phi - \phi_h\|_{\mathcal{Y}}^2 := \langle \mathcal{V}(\phi - \phi_h), \phi - \phi_h \rangle_\Gamma$. We stress that both coupling schemes recover the optimal convergence rate $\mathcal{O}(N^{-1/2})$ in the sum of the energy norms. However, the CFVM-BEM coupling has a stronger pre-refinement phase in $\|u - u_{FVM}\|_{\Omega}$, whereas all other norms are similar with respect to N .

Table 1 Energy norms for different refinement levels k for both coupling systems for example 5.1

k	Scheme	N	$\ u - u_{FVM}\ _{\Omega}$	$\ \xi - \xi_h\ _{\mathcal{H}}$	$\ \phi - \phi_h\ _{\mathcal{V}}$	$\ u - u_{FVM}\ _{L^2(\Omega)}$
8	FVM-BEM	1106	$1.70e - 02$	$4.85e - 03$	$4.72e - 03$	$9.90e - 05$
	CFVM-BEM	256	$2.96e - 02$	$2.83e - 02$	$2.41e - 02$	$9.67e - 04$
12	FVM-BEM	11592	$5.02e - 03$	$6.12e - 04$	$6.19e - 04$	$1.02e - 05$
	CFVM-BEM	1148	$8.25e - 03$	$4.63e - 03$	$4.20e - 03$	$1.22e - 04$
16	FVM-BEM	121544	$1.54e - 03$	$1.00e - 04$	$9.59e - 05$	$1.34e - 06$
	CFVM-BEM	9983	$2.39e - 03$	$1.03e - 03$	$8.13e - 04$	$1.28e - 05$
20	CFVM-BEM	94008	$7.44e - 04$	$1.74e - 04$	$1.69e - 04$	$1.61e - 06$



$\#\mathcal{T}^{(11)} = 6808.$



$\#\mathcal{T}^{(15)} = 5633.$

Fig. 1 Adaptively generated mesh for FVM-BEM (left) and CFVM-BEM (right) for example 5.1

Figure 1 shows adaptively refined meshes where we have chosen a mesh with almost the same number of elements. Both look similar. As expected the refinement happens around the singularity and a little bit on the coupling boundary.

5.2 A More Practical Example

Let us choose the same Ω as above and $\alpha = 0.1$, $\mathbf{b} = (15, 10)^T$ and $\gamma = 10^{-2}$. The volume force f is in the lower square, i.e., $f = 5$ for $-0.2 \leq x_1 \leq -0.1$, $-0.2 \leq x_2 \leq -0.05$ and $f = 0$ elsewhere. This example describes the stationary concentration of a chemical dissolved and distributed in a fluid, where we have a convection dominated problem in Ω and a diffusion distribution in Ω_e . This is a prototype of a transport problem but here without boundary conditions (which are “replaced” by the exterior problem). We prescribe the jumps $u_0 = 0$ and $t_0 = 0$ and fix the radiation condition $b_{\infty} = 0$ and get additionally the constraint $\int_{\Gamma} \phi_h ds = 2\pi b_{\infty}$. Note that we have an additional term $\langle a_{\infty}, \psi_h \rangle_{\Gamma}$ on the left-hand side of (2b) and (3c) with the unknown a_{∞} and an additional equation as the counterpart. In Fig. 2 we see that the refinement for both schemes happens from f along the convection \mathbf{b} and the layers at the boundary. However, the CFVM-BEM refinement is *more* local. The contour lines are generated at the same level and show the flow also into the unbounded domain and look very

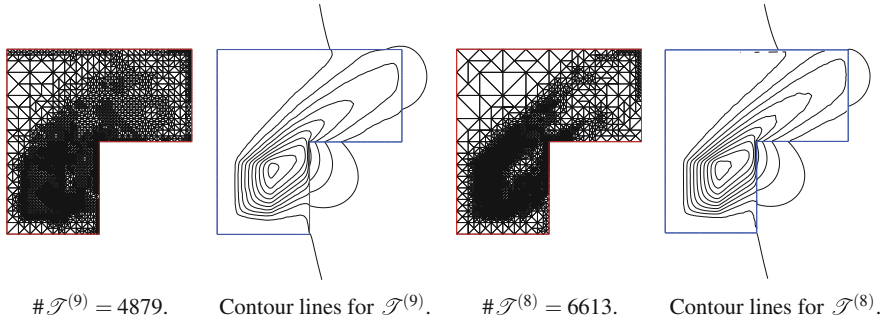


Fig. 2 Adaptively generated mesh and contour lines for FVM-BEM (left) and CFVM-BEM (right) for example 5.2

similar. The values in Ω_e can be calculated by the *representation formula* from the Cauchy data ξ_h and ϕ_h ; see [1, 2].

6 Conclusions

We have illustrated on practical experiments the effectiveness of both conservative adaptive coupling methods. Contrary to FEM-BEM couplings FVM-BEM and CFVM-BEM do not have a *global* Galerkin orthogonality which leads to some difficulties in their analysis. CFVM-BEM uses the primal mesh (local conservation of the fluxes) for the (non conforming) interior piecewise constant numerical solution, which could be an advantages for using meshes with hanging nodes. On the other hand CFVM-BEM has an additional block compared to FVM-BEM and one should do more tests to show the robustness of this additional interpolation. With an interior piecewise affine and globally continuous solution FEM-BEM is closer to the spirit of FEM-BEM but with the robustness of a finite volume scheme in the interior domain and mass conservation (but local fluxes on the dual mesh). The a posteriori estimation for CFVM-BEM is more complicated because it relies on a post processed Morley-type interpolant. Both a posteriori estimates are of residual type and robust and semi-robust in the upper and lower bound, respectively. More rigorous testing has to be done to recommend one over the other for a particular problem.

References

1. Erath, C.: Coupling of the finite volume element method and the boundary element method: an a priori convergence result. *SIAM J. Numer. Anal.* **50**(2), 574–594 (2012)
2. Erath, C.: A new conservative numerical scheme for flow problems on unstructured grids and unbounded domains. *J. Comput. Phys.* **245**, 476–492 (2013)

3. Erath, C.: A posteriori error estimates and adaptive mesh refinement for the coupling of the finite volume method and the boundary element method. *SIAM J. Numer. Anal.* **51**(3), 1777–1804 (2013)
4. Erath, C., Praetorius, D.: A posteriori error estimate and adaptive mesh refinement for the cell-centered finite volume method for elliptic boundary value problems. *SIAM J. Numer. Anal.* **47**(1), 109–135 (2008)